Neuro-Oncology Advances
5(1), 1–13, 2023 | https://doi.org/10.1093/noajnl/vdad092 | Advance Access date 21 July 2023

Imaging telomerase reverse transcriptase expression in oligodendrogliomas using hyperpolarized δ-[1-^{13}C]-gluconolactone

Georgios Batsios, Celine Taglang, Anne Marie Gillespie, and Pavithra Viswanath

Department of Radiology and Biomedical Imaging, University of California San Francisco, San Francisco, California, USA (G.B., C.T., A.M.G., P.V.)

Corresponding Author: Pavithra Viswanath, PhD, 1700 4th St, Byers Hall, Suite BH303E, San Francisco, CA 94143, USA (Pavithra.Viswanath@ucsf.edu).

Abstract

Background. Telomere maintenance by telomerase reverse transcriptase (TERT) is essential for immortality in most cancers, including oligodendrogliomas. Agents that disrupt telomere maintenance such as the telomere uncapping agent 6-thio-2′-deoxyguanosine (6-thio-dG) are in clinical trials. We previously showed that TERT expression in oligodendrogliomas is associated with upregulation of glucose-6-phosphate dehydrogenase (G6PD), the rate-limiting enzyme of the pentose phosphate pathway (PPP). We also showed that hyperpolarized δ-[1-^{13}C]-gluconolactone metabolism to 6-phosphogluconate (6-PG) can be used to probe the PPP in glioblastomas. The goal of this study was to determine whether hyperpolarized ^{13}C imaging using δ-[1-^{13}C]-gluconolactone can monitor TERT expression and response to 6-thio-dG in oligodendrogliomas.

Methods. We examined patient-derived oligodendroglioma cells and orthotopic tumors to assess the link between TERT and hyperpolarized δ-[1-^{13}C]-gluconolactone metabolism. We performed in vivo imaging to assess the ability of hyperpolarized δ-[1-^{13}C]-gluconolactone to report on TERT and response to 6-thio-dG in rats bearing orthotopic oligodendrogliomas in vivo.

Results. Doxycycline-inducible TERT silencing abrogated 6-PG production from hyperpolarized δ-[1-^{13}C]-gluconolactone in oligodendroglioma cells, consistent with the loss of G6PD activity. Rescuing TERT expression by doxycycline removal restored G6PD activity and, concomitantly, 6-PG production. 6-PG production from hyperpolarized δ-[1-^{13}C]-gluconolactone demarcated TERT-expressing tumor from surrounding TERT-negative normal brain in vivo. Importantly, 6-thio-dG abrogated 6-PG production at an early timepoint preceding MRI-detectable alterations in rats bearing orthotopic oligodendrogliomas in vivo.

Conclusions. These results indicate that hyperpolarized δ-[1-^{13}C]-gluconolactone reports on TERT expression and early response to therapy in oligodendrogliomas. Our studies identify a novel agent for imaging tumor proliferation and treatment response in oligodendroglioma patients.

Key Points

- Hyperpolarized δ-[1-^{13}C]-gluconolactone can probe G6PD activity in oligodendrogliomas.
- Hyperpolarized δ-[1-^{13}C]-gluconolactone informs on telomerase reverse transcriptase and treatment response in vivo.

Telomere maintenance is a fundamental hallmark of cancer.[1,2] Telomeres are cap-like structures composed of telomeric DNA and specialized proteins that protect the ends of linear chromosomes from damage during DNA replication.[2] Telomeres shorten with every cell division until the cell undergoes senescence.[1,2] To achieve replicative immortality, tumor cells need a mechanism for maintaining telomere length. Most tumors (~85%) reactivate expression of telomerase reverse

Importance of the Study

MRI is the mainstay for glioma patient management. However, oligodendrogliomas are difficult to visualize by MRI. Importantly, MRI fails to adequately report on response to therapy. There is a need for noninvasive methods that can be used to visualize oligodendrogliomas and their response to therapy. Telomerase reverse transcriptase (TERT) expression is essential for telomere maintenance and is a fundamental event in oligodendroglioma formation. TERT is also an attractive therapeutic target and the drug 6-thio-2′-deoxyguanosine that disrupts telomere maintenance is in clinical trials for cancer. We previously showed that TERT expression is associated with upregulation of the pentose phosphate pathway (PPP) in oligodendrogliomas. Here, we have established the ability of hyperpolarized δ-[1-^{13}C]-gluconolactone, a novel probe of the PPP, to assess TERT expression and response to 6-thio-2′-deoxyguanosine in oligodendroglioma models in vivo. Our findings identify a noninvasive method of imaging as a hallmark of cancer and have the potential to improve management of oligodendroglioma patients.

transcriptase (TERT), which is the catalytic component of the enzyme telomerase that synthesizes telomeric DNA.[2,3] Reactivation of TERT expression occurs via hotspot mutations in the TERT promoter that facilitate recruitment of the transcription factor GA-binding protein specifically in cancer cells.[3–5] In contrast, TERT expression is silenced early in development in normal somatic cells, except stem cells where it is maintained via the wild-type TERT promoter.[2,3]

Oligodendrogliomas are solid primary brain tumors characterized by the presence of an isocitrate dehydrogenase mutation combined with a chromosomal 1p/19q codeletion.[6] TERT promoter mutations are observed in >90% of oligodendrogliomas, suggesting that TERT has potential as an additional diagnostic marker.[7,8] Due to the specificity of TERT promoter mutations to cancer and the key role of TERT in sustaining tumor proliferation, TERT is an attractive therapeutic target.[2,3] Disruption of TERT expression from the mutant TERT promoter prolongs survival in mice bearing orthotopic gliomas, pointing to a potential therapeutic strategy.[5] Another promising therapeutic strategy is the use of telomere uncapping agents such as 6-thio-2′-deoxyguanosine (6-thio-dG).[9–12] 6-thio-dG causes telomeric DNA damage and cell death in TERT-expressing tumor cells but not TERT-negative tumor cells or normal astrocytes.[9–12] Importantly, 6-thio-DG is currently in clinical trials for solid tumors (NCT05208944).

Oncogenic events reprogram tumor metabolism in order to generate the biosynthetic and bioenergetic intermediates needed to sustain uncontrolled proliferation.[1] For instance, glucose metabolism via the pentose phosphate pathway (PPP) is the major source of NADPH, which is essential for redox maintenance, and of ribulose-5-phosphate, which is a structural component of nucleotides.[13] The PPP begins with the oxidation of glucose-6-phosphate to 6-phospho-δ-gluconolactone with the concomitant reduction of NADP+ to NADPH by the rate-limiting enzyme glucose-6-phosphate dehydrogenase (G6PD; see Figure 1A). 6-phospho-δ-gluconolactone is then hydrolyzed to 6-phosphogluconate (6-PG) by 6-phosphogluconolactonase (PGLS). 6-PG is subsequently converted to ribulose-5-phosphate by 6-phosphogluconate dehydrogenase, in a reaction that also generates NADPH. Importantly, we previously demonstrated that TERT expression is associated with elevated steady-state levels of glutathione and NADPH.[14,15] NADPH maintains glutathione in the reduced state and we showed that silencing TERT leads to loss of NADPH, glutathione, and elevated oxidative stress.[14,15] Mechanistically, TERT upregulates glucose flux via the PPP by activating the sirtuin SIRT2 which, in turn, upregulates G6PD expression and activity in oligodendroglioma cells and rats bearing orthotopic tumors.[14]

Magnetic resonance spectroscopy (MRS) is a noninvasive, non-radioactive method of imaging tissue metabolism in real-time in vivo.[16] ^{1}H-MRS measures steady-state metabolite levels and is used in clinical research.[16] However, ^{1}H-MRS does not detect metabolites of the PPP, nor does it provide a readout of PPP activity. Thermally polarized ^{13}C-MRS following administration of ^{13}C-labeled precursors such as [2-^{13}C]-glucose can trace metabolic fluxes, but suffers from low sensitivity which limits clinical translatability.[16] The implementation of hyperpolarized ^{13}C-MRS has enhanced the signal-to-noise ratio (SNR) of ^{13}C-MRS by >10 000 fold, thereby providing a noninvasive method of imaging dynamic metabolic fluxes in vivo.[17,18] Importantly, the feasibility of hyperpolarized ^{13}C-MRS has been established in patients with gliomas and other cancers.[17,18] In the context of the PPP, we recently demonstrated that hyperpolarized δ-[1-^{13}C]-gluconolactone can monitor the activity of the second PPP enzyme PGLS in preclinical glioblastoma models in vivo.[19] Following entry via the glucose transporters,[20,21] hyperpolarized δ-[1-^{13}C]-gluconolactone is rapidly phosphorylated by gluconokinase to 6-phospho-δ-[1-^{13}C]-gluconolactone and converted to 6-PG[20–22] (see Figure 1A).

Since TERT is essential for tumor proliferation, noninvasive methods of imaging TERT have the potential to report on tumor burden and response to therapy in vivo. As detailed above, our previous studies indicate that TERT upregulates G6PD expression and glucose flux via the PPP.[14] Since G6PD functions upstream of PGLS and is a rate-limiting enzyme, hyperpolarized δ-[1-^{13}C]-gluconolactone has the potential to provide a readout of TERT-linked G6PD activity in vivo. Therefore, the goal of this study was to evaluate whether hyperpolarized δ-[1-^{13}C]-gluconolactone can assess TERT-associated upregulation of G6PD in oligodendrogliomas in vivo. Our findings indicate that 6-PG production from hyperpolarized

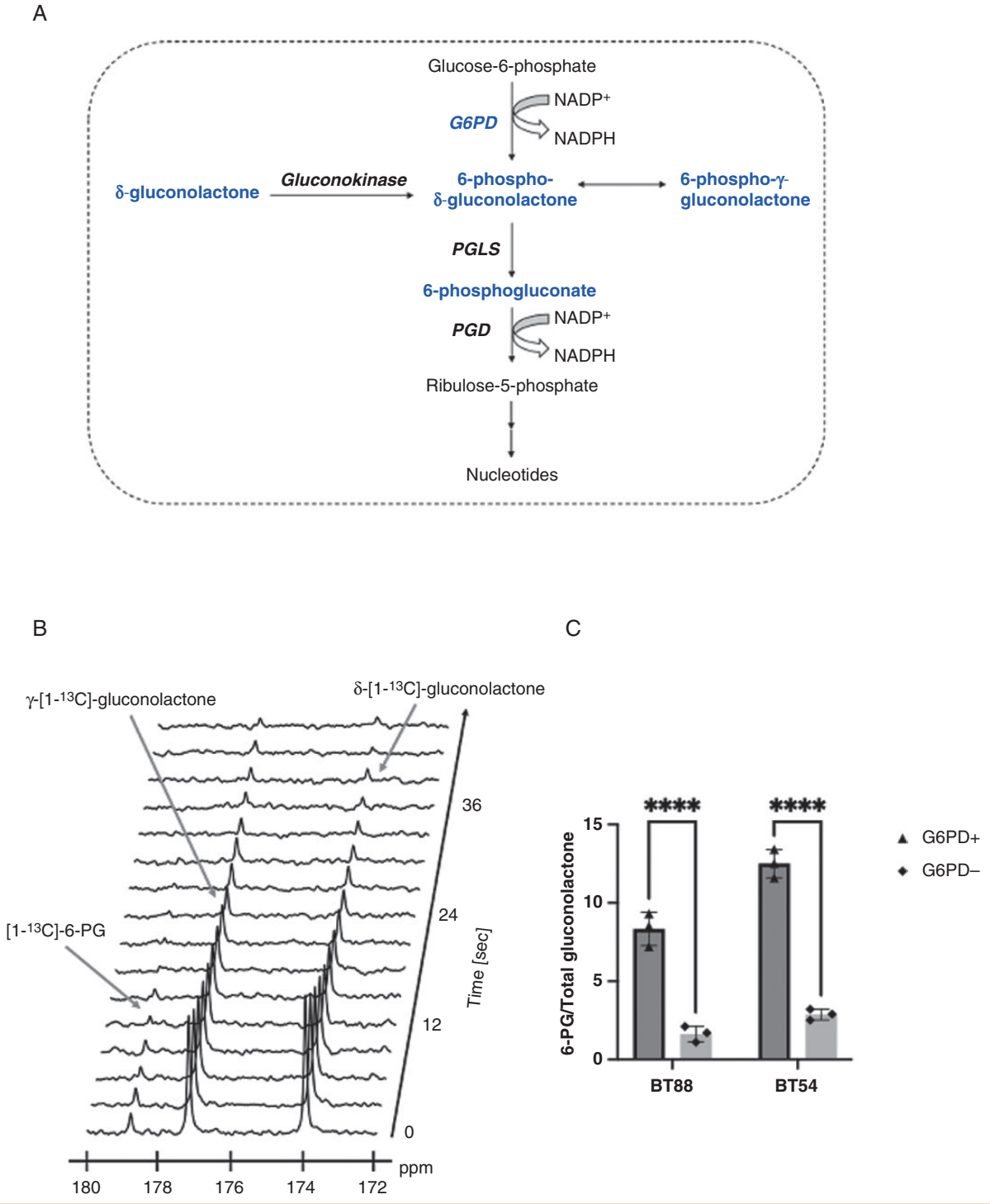

Figure 1. Hyperpolarized δ-[1-^{13}C]-gluconolactone metabolism to [1-^{13}C]-6-PG reports on G6PD in patient-derived oligodendroglioma cells. (A) Schematic illustration of the pentose phosphate pathway (PPP). G6PD is the rate-limiting enzyme of the PPP and converts glucose-6-phosphate to 6-phospho-δ-gluconolactone, which is in equilibrium with 6-phospho-γ-gluconolactone. δ-gluconolactone is converted to 6-phospho-δ-gluconolactone by gluconokinase. PGLS converts 6-phospho-δ-gluconolactone to 6-PG. PGD converts 6-PG to ribulose-5-phosphate, which is the precursor for nucleotide biosynthesis. G6PD: Glucose-6-phosphate dehydrogenase; PGLS, 6-phosphogluconolactonase; PGD: 6-phosphogluconate dehydrogenase. 6-PG: 6-phosphogluconate. (B) Representative ^{13}C-MR spectral array showing dynamic production of [1-^{13}C]-6-PG from hyperpolarized δ-[1-^{13}C]-gluconolactone in live BT88 cells. The peaks for δ-[1-^{13}C]-gluconolactone (173.8 ppm), γ-[1-^{13}C]-gluconolactone (177 ppm), and [1-^{13}C]-6-PG (178.6 ppm) are labeled. (C) Effect of G6PD silencing on the ratio of [1-^{13}C]-6-PG to total [1-^{13}C]-gluconolactone in the BT88 and BT54 models ($n = 3$ each). **** indicates statistical significance with $P < .0001$.

δ-[1-^{13}C]-gluconolactone provides a readout of TERT expression in oligodendrogliomas. Importantly, 6-PG production from hyperpolarized δ-[1-^{13}C]-gluconolactone reports on early response to 6-thio-dG in vivo.

Materials and Methods

Cell Culture

The BT54 and BT88 cell lines were kind gifts from Dr. Luchman and Dr. Cairncross from the University of Calgary, Alberta, Canada. The SF10417 model was a kind gift from Dr. Joseph Costello from the University of California San Francisco. BT54 cells were derived from a patient carrying a WHO grade III oligodendroglioma.[23] SF10417 and BT88 cells were isolated from male patients harboring oligodendrogliomas.[23,24] BT54 were grown as neurospheres in Neurocult medium (Stem Cell Technologies) supplemented with epidermal growth factor (20 ng/mL, Peprotech), fibroblast growth factor 2 (20 ng/mL, Peprotech) and heparin sulphate (2 mg/mL; Stem Cell Technologies).[23,25–27] SF10417 cells were maintained as monolayers in laminin-coated flasks and were cultured in serum-free Neurocult NS-A medium containing 2 mM glutamine, 1% penicillin/streptomycin, B-27 and N2 supplements, 20 ng/mL epidermal growth factor, 20 ng/mL fibroblast growth factor 2 and 20 ng/mL platelet-derived growth factor-AA.[14,15,24] BT88 cells were maintained as monolayers in Dulbecco's Modified Eagles medium supplemented with 2 mM glutamine, 10% fetal calf serum, and 1% penicillin/streptomycin. Cell lines were routinely tested for mycoplasma contamination, authenticated by short tandem repeat fingerprinting (Cell Line Genetics), and assayed within 6 months of authentication.

Gene Silencing

Expression of *TERT*, *G6PD*, *PGLS,* and gluconokinase (gene ID: *IDNK*, or C9orf103) was silenced using RNA interference as described previously.[14,15,19] Briefly, ~2 × 10^6 cells were seeded in a 150 mm dish and allowed to adhere for 24 hours. Cells were then transfected with 25 nM siRNA using the DharmaFECT 4 transfection reagent (Dharmacon) and incubated at 37°C for an additional 72 hours prior to harvesting for further studies. Silencing was carried out using siGENOME SMARTpool siRNA (*TERT*: catalog # M-003547-02; *IDNK*: catalog # M-032285-00; G6PD: catalog # M-008181-02; PGLS: catalog # M-020023-00). siGENOME non-targeting siRNA Pool #2 was used as control (catalog # D-001206-14). The doxycycline-inducible TERT silencing construct has been previously described.[28] Briefly, microRNA-embedded miR-E shRNA against TERT was cloned into a lentiviral vector (pCW57-TurboGFP-miR-E-puro). Lentiviral particles were produced by transient transfection of psPAX2 (Addgene #12260), pMD2.G (Addgene #12259), and transfer plasmid (pCW57-CMV-GFP-miR-E-IRES-puro-shRNA) into HEK293T cells. BT88 cells were transduced with lentivirus followed by puromycin selection. For silencing, cells were treated with 0.4 μg/mL of doxycycline for 24 hours. For rescue of TERT expression, cells were treated with 0.4 μg/mL of doxycycline for 24 hours, washed with saline, and grown in doxycycline-free media for 48 hours before examination.

Expression and Activity Assays

Gene expression was confirmed by quantitative RT-PCR.[14,15] Briefly, the SYBR Green Quantitative RT-PCR Kit (Sigma-Aldrich) was used with the following primers: TERT (forward primer: TCACGGAGACCACGTTTCAAA; reverse primer: TTCAAGTGCTGTCTGATTCCAAT), G6PD (forward primer: TGAGCCAGATAGGCTGGAA; reverse primer: TAACGCAGGCGATGTTGTC), PGLS (forward primer: TGTGGCAACTGGAGAAGGCAAG; reverse primer: CTCGTCCAAGAACCAGCACAGT) and IDNK (forward primer: GAAAAGGCATACCGCTCAAT; reverse primer: GAGATGACCTCAAACGACCC). β-actin (forward primer: AGAGCTACGAGCTGCCTGAC; reverse primer: AGCACTGTGTTGGCGTACAG) was used as control for normalization. Telomerase activity was quantified using the telomeric repeat amplification protocol assay, (TRAPeze® RT kit, Sigma) which is the gold standard for measurement of telomerase activity.[29,30] The effect of TERT silencing on G6PD activity was measured using a kit according to manufacturer's instructions (Abcam, ab102529).

Hyperpolarized ^{13}C-MRS of Live Cells

Hyperpolarized δ-[1-^{13}C]-gluconolactone was synthesized and polarized as described previously.[19] Briefly, 2M δ-[1-^{13}C]-gluconolactone was dissolved in 3:1 water:glycerol, mixed with 15 mM OX063 trityl radical and polarized in a HyperSense polarizer. We previously showed that hyperpolarized δ-[1-^{13}C]-gluconolactone has a T1 of 31.7 ± 4.7 seconds at 3T.[19] After maximal polarization was achieved, the sample was dissolved in phosphate-buffered saline (pH ~7) to a final concentration of 8mM and added to a suspension of live cells.[14,15,19] ^{13}C spectra were acquired on a 11.7T Varian or a 14.1T Bruker spectrometer with a 13° flip angle every 3 seconds for 300 seconds. Data analysis were performed using Mnova (MestreLab). δ-gluconolactone is in equilibrium with γ-gluconolactone in aqueous solutions and we previously confirmed that differences in the relative levels of δ- and γ-gluconolactone did not influence 6-PG production.[19] Therefore, we evaluated the ratio of [1-^{13}C]-6-PG to the combined signal from hyperpolarized δ-[1-^{13}C]-gluconolactone and γ-[1-^{13}C]-gluconolactone (henceforth referred to as total [1-^{13}C]-gluconolactone) and to cell number.

MRI

Animal studies were conducted in accordance with UCSF Institutional Animal Care and Use Committee guidelines. SF10417 or BT88 (2 × 10^5 or 3 × 10^5 cells, respectively in 10 μL) were intracranially injected into athymic male nude rats (5–6 weeks).[14,15,19] T2-weighted MRI was performed on a horizontal Bruker 3T scanner equipped with a dual-tuned ^{1}H-^{13}C linear-linear volume coil (40 mm inner diameter;

Bruker) or a dual-tuned ^{1}H-^{13}C quadrature-quadrature volume coil (45 mm inner diameter; NeosBiotec) using a spin echo TurboRARE sequence (TE/TR = 64/3484 ms, FOV = 43 × 43mm^2, 256 × 256, slice thickness = 1 mm, NA = 6). Tumors were manually segmented, and tumor volume was determined as a sum of the areas multiplied by slice thickness. For assessment of response to 6-thio-dG, rats bearing orthotopic BT88 tumors were examined. Once tumors reached a volume of 64.8 ± 36.1mm^3, this timepoint was considered day 0, and hyperpolarized δ-[1-^{13}C]-gluconolactone metabolism was evaluated as described below. Rats were then treated intraperitoneally with 6-thio-dG (50 mg/kg in saline) daily for 7 days and then treated 4 times every week. Treatment was continued until tumors were no longer visible on MRI.

Hyperpolarized ^{13}C-MRS In Vivo

Following polarization, 2.2 mL of hyperpolarized δ-[1-^{13}C]-gluconolactone corresponding to a final concentration of 37.8 mM was injected via a tail-vein catheter over 12 seconds. For non-localized slab studies, rats bearing orthotopic SF10417 tumors or tumor-free healthy controls were examined. Dynamic ^{13}C spectra were acquired using the 40 mm Bruker coil from a 12 mm axial slab through the brain every 3 seconds using a flyback spectral-spatial RF pulse with flip angles of 15.3° on [1-^{13}C]-6-PG, 3.4° on δ-[1-^{13}C]-gluconolactone and 12° on γ-[1-^{13}C]-gluconolactone. ^{13}C slab spectra were analyzed using Mnova and the SNR for [1-^{13}C]-6-PG, δ-[1-^{13}C]-gluconolactone and γ-[1-^{13}C]-gluconolactone quantified. We compared the ratio of [1-^{13}C]-6-PG to total [1-^{13}C]-gluconolactone and the SNR of total-[1-^{13}C]-gluconolactone between tumor-bearing and tumor-free rats. For spatial localization, data were acquired using the 45 mm NeosBiotec coil and a 2D flyback spectral-spatial echo-planar spectroscopic imaging (EPSI) sequence with flip angles as described above.[19] The spatial resolution of the EPSI method was 5.375 × 5.375 × 8mm^3, the temporal resolution was 3 seconds, and the spectral resolution was 128 points over 20 ppm. 2D EPSI data were analyzed using in-house MATLAB codes available from a GitHub repository (https://github.com/ViswanathLab/EPSI).[14,15,19] For each voxel at every time point, spectra were analyzed after a 5 Hz line broadening, peak integrals were evaluated and the SNR was calculated by normalizing to noise, which was evaluated as the standard deviation of the real part of the signal in a voxel outside of the brain.[14,15,19] Color heatmaps were generated by interpolating the raw data using the Lanczos-2 interpolation algorithm.[14,15,19]

Statistics

All experiments were performed on a minimum of 3 samples ($n \geq 3$) and results were presented as mean ± standard deviation. Statistical analyses were performed using GraphPad Prism 9. For cell studies and in vivo slab studies, statistical significance was assessed using an unpaired Welch's two-tailed *t*-test assuming unequal variance with $P < .05$ considered significant. A paired one-tailed *t*-test was used to assess the statistical significance of differences between tumor and contralateral normal brain in 2D EPSI studies. An ordinary two-way ANOVA (uncorrected Fisher's LSD) was used to assess the statistical significance of differences between day 0 and day 7 of treatment in tumor versus contralateral normal brain in 2D EPSI studies. * indicates statistical significance with $P < .05$, ** indicates statistical significance with $P < .01$, *** indicates statistical significance with $P < .001$ and **** indicates statistical significance with $P < .0001$.

Results

Hyperpolarized δ-[1-^{13}C]-Gluconolactone Reports on TERT-Mediated Upregulation of G6PD in Oligodendroglioma Cells

Our prior studies indicate that silencing TERT downregulates G6PD expression and activity and reduces glucose flux via the PPP in genetically engineered and patient-derived oligodendroglioma cells.[14] Although G6PD functions upstream of PGLS, nevertheless, it is the rate-limiting enzyme of the PPP. Rate-limiting enzymes are known to influence flux via the entire metabolic pathway.[31,32] Therefore, hyperpolarized δ-[1-^{13}C]-gluconolactone has the potential to report on TERT-mediated upregulation of G6PD in oligodendrogliomas. To clearly delineate the link between TERT and hyperpolarized δ-[1-^{13}C]-gluconolactone, we examined the expression of the various components involved in hyperpolarized δ-[1-^{13}C]-gluconolactone metabolism in TERT+ and TERT– cells. Hyperpolarized δ-[1-^{13}C]-gluconolactone is phosphorylated to 6-phospho-δ-[1-^{13}C]-gluconolactone by gluconokinase (see Figure 1A). 6-phospho δ-[1-^{13}C]-gluconolactone is then converted to 6-PG by the action of PGLS. We confirmed that there is no difference in gluconokinase or PGLS expression between TERT+ and TERT– cells for both BT88 and BT54 oligodendroglioma models (Supplementary Figure S1A-S1B). To directly confirm that hyperpolarized δ-[1-^{13}C]-gluconolactone provides a readout of G6PD activity, we examined the effect of G6PD silencing on hyperpolarized δ-[1-^{13}C]-gluconolactone metabolism in oligodendroglioma cells. As shown in Figure 1B, following addition to a suspension of live BT88 cells, hyperpolarized δ-[1-^{13}C]-gluconolactone (173.8 ppm) metabolism to [1-^{13}C]-6-PG (178.6 ppm) was clearly observed. In line with previous studies,[19,20] we also observed a peak for γ-[1-^{13}C]-gluconolactone (177 ppm), which is in equilibrium with δ-[1-^{13}C]-gluconolactone in aqueous solutions. Importantly, G6PD silencing (see Supplementary Figure S1C-S1D for verification of loss of G6PD expression and activity) significantly reduced 6-PG production from hyperpolarized δ-[1-^{13}C]-gluconolactone in both BT88 and BT54 models (Figure 1C).

We then examined whether hyperpolarized δ-[1-^{13}C]-gluconolactone has the ability to provide a readout of TERT-mediated upregulation of G6PD in patient-derived oligodendroglioma cells. As shown in Figure 2A, silencing TERT by RNA interference (see Supplementary Figure S1E-S1F for verification of loss of TERT expression and telomerase activity) significantly reduced 6-PG production from hyperpolarized δ-[1-^{13}C]-gluconolactone in both BT88 and

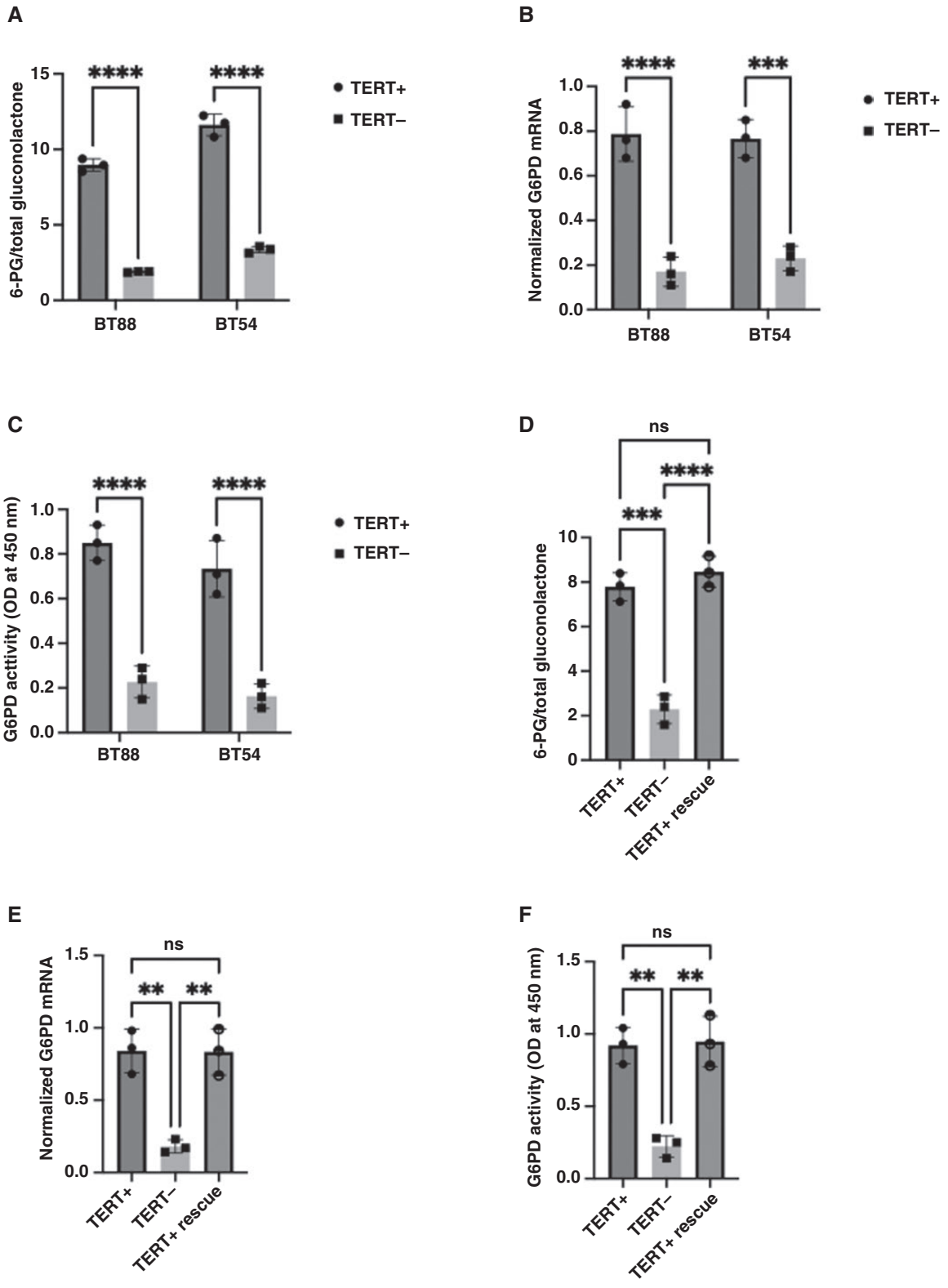

Figure 2. Hyperpolarized δ-[1-^{13}C]-gluconolactone provides a readout of TERT expression in patient-derived oligodendroglioma cells. The effect of silencing TERT on (A) the ratio of [1-^{13}C]-6-PG to total [1-^{13}C]-gluconolactone (B) G6PD mRNA and (C) G6PD activity in the BT88 and BT54 models ($n = 3$ each). Ratio of [1-^{13}C]-6-PG to total [1-^{13}C]-gluconolactone (D), G6PD mRNA (E), and G6PD activity (F) in BT88 cells with doxycycline-inducible TERT expression. TERT+ refers to BT88 cells treated with saline, TERT– indicates cells treated with doxycycline, and TERT+ rescue refers to cells in which TERT expression was rescued by doxycycline removal. ** indicates statistical significance with $P < .01$, *** indicates statistical significance with $P < .001$ and **** indicates statistical significance with $P < .0001$. ns indicates a lack of statistical significance.

BT54 models. These results are consistent with the significant reduction in G6PD expression and activity in TERT– cells relative to TERT+ (Figure 2B-2C). To further confirm that hyperpolarized δ-[1-^{13}C]-gluconolactone can reliably track TERT expression with serial silencing and reactivation over time, we examined BT88 cells in which TERT expression could be silenced in a doxycycline-inducible manner (see Supplementary Figure S2A-S2B for verification of loss of TERT expression and telomerase activity). Our studies indicate that 6-PG production from hyperpolarized δ-[1-^{13}C]-gluconolactone is abrogated upon doxycycline-mediated TERT silencing and restored upon rescue of TERT expression via doxycycline removal (Figure 2D). Concomitantly, G6PD expression and activity are significantly reduced upon doxycycline-mediated TERT silencing and restored upon TERT rescue by doxycycline removal (Figure 2E–F). Collectively, our studies indicate that 6-PG production from hyperpolarized δ-[1-^{13}C]-gluconolactone is a biomarker of TERT expression in patient-derived oligodendroglioma cells.

Hyperpolarized δ-[1-^{13}C]-Gluconolactone Metabolism to 6-PG Reports on TERT Expression in Oligodendrogliomas In Vivo

We previously showed that hyperpolarized δ-[1-^{13}C]-gluconolactone metabolism can be observed in the normal brain in vivo.[19] Here, we examined the test–retest repeatability of 6-PG production in the brain of healthy, tumor-free rats. In accordance with the guidelines for quantitative imaging studies,[33] we measured the within-subject coefficient of variation (wCV) in EPSI studies performed on two consecutive days. Our results (Supplementary Figure S2C-S2D) indicate that the wCV of 6-PG production in vivo is 13.9%, which is in line with values reported for other imaging methods such as FDG-PET, ^{1}H-MRS, and hyperpolarized [1-^{13}C]-pyruvate.[34–36]

Next, we examined the feasibility of imaging TERT in vivo using hyperpolarized δ-[1-^{13}C]-gluconolactone. Dynamic ^{13}C spectra were acquired from a 12 mm slab through the brain of rats bearing orthotopic TERT+ SF10417 tumors or tumor-free controls following intravenous injection of hyperpolarized δ-[1-^{13}C]-gluconolactone (see Supplementary Figure S2E–S2F for confirmation of TERT expression and telomerase activity in tumor vs. normal brain). As shown in Figure 3A–B, consistent with our cell studies, 6-PG production was significantly higher in rats bearing TERT+ SF10417 tumors relative to TERT- normal brains. In contrast, there was no significant difference in the SNR of total [1-^{13}C]-gluconolactone (Figure 3C), indicating that the differences in 6-PG production between tumor and normal brain were not the result of differences in gluconolactone delivery.

To further confirm these results and assess the spatial distribution of 6-PG production, we performed 2D EPSI following intravenous administration of hyperpolarized δ-[1-^{13}C]-gluconolactone to rats bearing orthotopic BT88 tumors. Representative ^{13}C-MR spectra from voxels placed over tumor or contralateral normal brain in a rat bearing an orthotopic BT88 tumor are shown in Figure 4A. Visualization of the data in the form of metabolic heatmaps generated by overlaying metabolic data over the corresponding MRI showed localization of 6-PG to the tumor while gluconolactone was distributed homogenously over the brain (Figure 4B and Supplementary Figure S3). Importantly, consistent with the non-localized slice-selective studies, the SNR of [1-^{13}C]-6-PG was significantly higher in the tumor relative to the contralateral normal brain while there was no difference in the SNR of total [1-^{13}C]-gluconolactone (Figure 4C–D). Collectively, these results suggest that 6-PG production from hyperpolarized δ-[1-^{13}C]-gluconolactone is a biomarker of TERT expression in vivo and point to its ability to demarcate tumors from normal brain in patient-derived oligodendroglioma models.

Hyperpolarized δ-[1-^{13}C]-Gluconolactone Reports on Early Response to Therapy in Oligodendrogliomas In Vivo

Having established the ability of hyperpolarized δ-[1-^{13}C]-gluconolactone to differentiate tumor from normal brain, we then assessed its ability to inform on response to therapy. 6-thio-dG is a nucleoside analog that is recognized and incorporated by telomerase, disrupts telomeres, and induces cell death in TERT+ cancers.[9–12] We treated rats bearing orthotopic BT88 tumors with 6-thio-dG and examined hyperpolarized δ-[1-^{13}C]-gluconolactone metabolism by 2D EPSI before (day 0) and after (day 7) treatment. As shown in the representative spectra in Figure 5A, 6-PG production was significantly reduced at day 7 relative to day 0. Visualization of the data in the form of metabolic heatmaps confirmed the reduction in 6-PG production in the tumor at day 7 relative to day 0 (Figure 5B). In contrast, there was no difference in spatial distribution of total [1-^{13}C]-gluconolactone at day 7 vs. day 0 (Figure 5B). Quantification of the SNR of [1-^{13}C]-6-PG and total [1-^{13}C]-gluconolactone confirmed the statistical significance of these results (Figure 5C–D). Importantly, 6-thio-dG significantly reduced tumor volume only at day 14 (Figure 5E), indicating that the reduction in 6-PG production precedes tumor shrinkage. Collectively, our results indicate that 6-PG production from hyperpolarized δ-[1-^{13}C]-gluconolactone is a biomarker of response to 6-thio-dG at early time points that precede the onset of MRI-detectable anatomical alterations in vivo.

Discussion

Telomere maintenance is essential for tumor proliferation.[1,2] Most human tumors, including oligodendrogliomas, maintain telomere length via reactivation of TERT expression. noninvasive detection of TERT has the potential to provide a readout of tumor proliferation and response to therapy. Here, we show that 6-PG production from hyperpolarized δ-[1-^{13}C]-gluconolactone is a metabolic imaging biomarker of TERT expression and response to therapy in oligodendrogliomas.

At present, detection of TERT expression requires Sanger sequencing, pyrosequencing, and quantitative or droplet

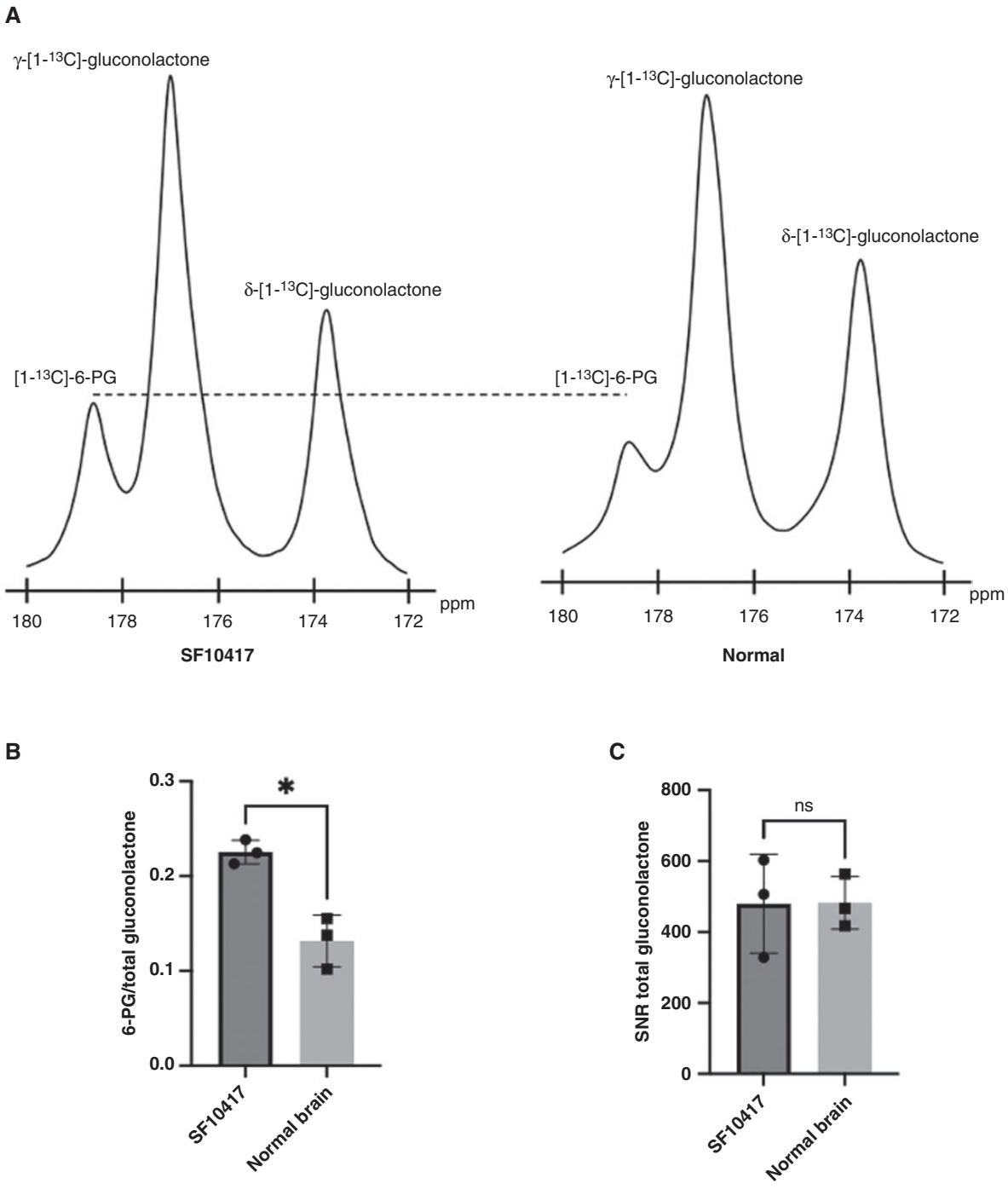

Figure 3. Hyperpolarized δ-[1-^{13}C]gluconolactone metabolism to 6-PG can be noninvasively monitored in patient-derived oligodendroglioma models in vivo. (A) Representative summed ^{13}C-MR spectra showing [1-^{13}C]-6-PG production from hyperpolarized δ-[1-^{13}C]-gluconolactone in a rat bearing an orthotopic SF10417 tumor (left panel) or tumor-free control (right panel). Spectra were acquired from a slab through the brain following intravenous administration of hyperpolarized δ-[1-^{13}C]-gluconolactone. Peaks for δ-[1-^{13}C]-gluconolactone (173.8 ppm), γ-[1-^{13}C]-gluconolactone (177 ppm), and [1-^{13}C]-6-PG (178.6 ppm) are labeled. The dotted line highlights the higher 6-PG signal in the tumor-bearing rat. Quantification of the ratio of [1-^{13}C]-6-PG to total [1-^{13}C]-gluconolactone (B) and the signal-to-noise ratio of total [1-^{13}C]-gluconolactone (C) in SF10417 tumor-bearing and tumor-free rats ($n = 3$ each). * indicates statistical significance with $P < .05$. ns indicates a lack of statistical significance.

digital PCR of tumor biopsies.[37,38] However, the infiltrative nature, anatomical location, and the complications of repeated neurosurgery make it difficult to longitudinally monitor TERT expression using biopsy-based methods. Although liquid biopsies provide an alternate, minimally invasive approach, the blood-brain barrier remains a

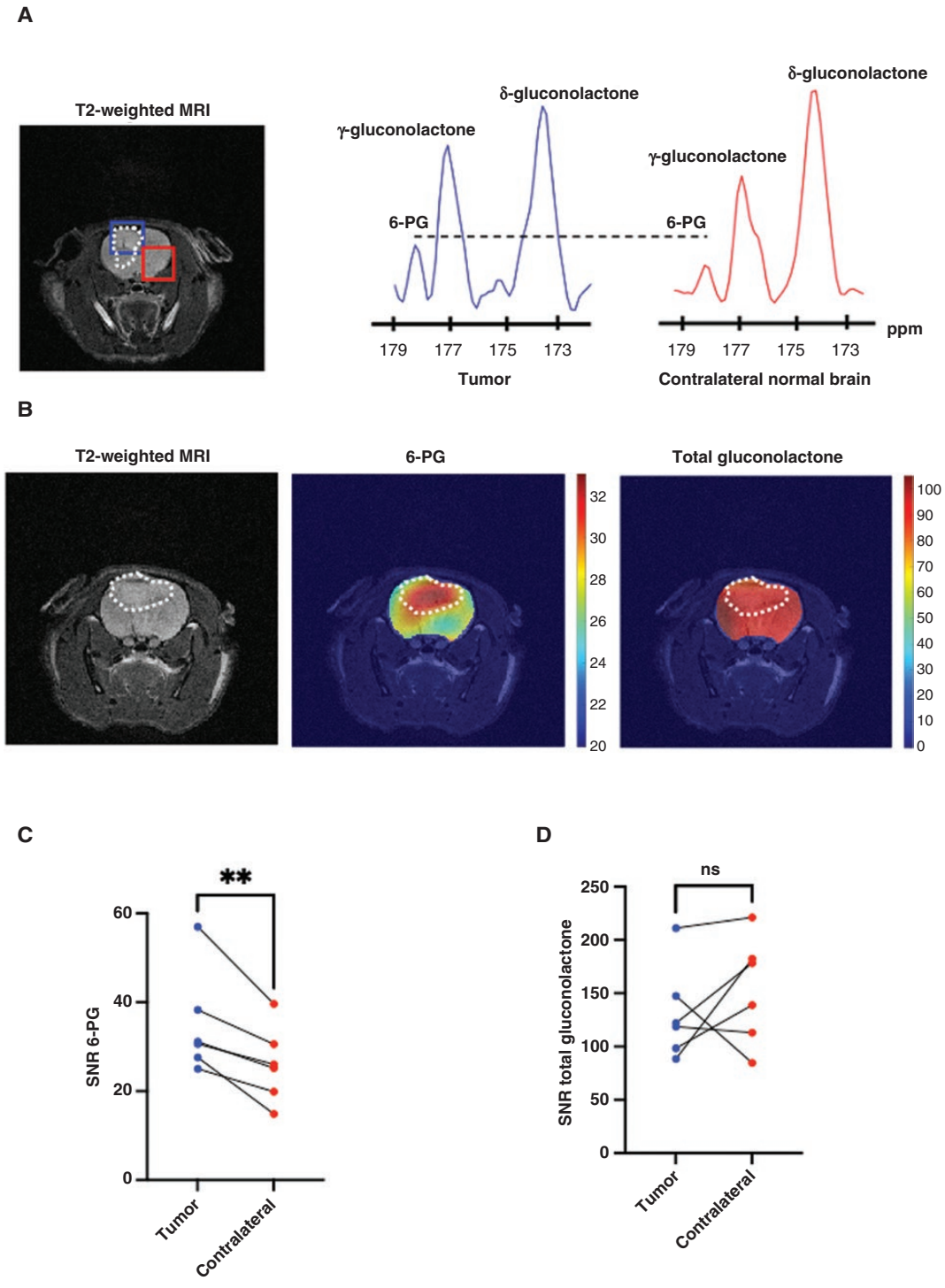

Figure 4. Hyperpolarized δ-[1-^{13}C]-gluconolactone metabolism can be used to monitor tumor burden in oligodendrogliomas in vivo. (A) Representative 2D echo-planar spectroscopic imaging (EPSI) data showing the T2-weighted MRI (left panel) and corresponding ^{13}C-MR spectra (right panel) from voxels placed over the tumor or contralateral normal brain in a rat bearing an orthotopic BT88 tumor. Tumor voxel and spectra are shown in blue and contralateral normal brain voxel and spectra are in red. The tumor region is contoured by white dotted lines. (B) Representative heatmaps from 2D EPSI in a rat bearing an orthotopic BT88 tumor. The left panel shows a T2-weighted MRI with the tumor contoured in white. The middle panel shows the heatmap of the signal-to-noise ratio (SNR) of [1-^{13}C]-6-PG overlaid over the T2-weighted MRI. The right panel shows the heatmap of the SNR of total [1-^{13}C]-gluconolactone overlaid over the T2-weighted MRI. Quantification of the SNR of [1-^{13}C]-6-PG (C) and the SNR of total [1-^{13}C]-gluconolactone (D) in tumor relative to normal brain in rats bearing orthotopic BT88 tumors ($n = 6$). ** indicates statistical significance with $P < .01$. ns indicates a lack of statistical significance.

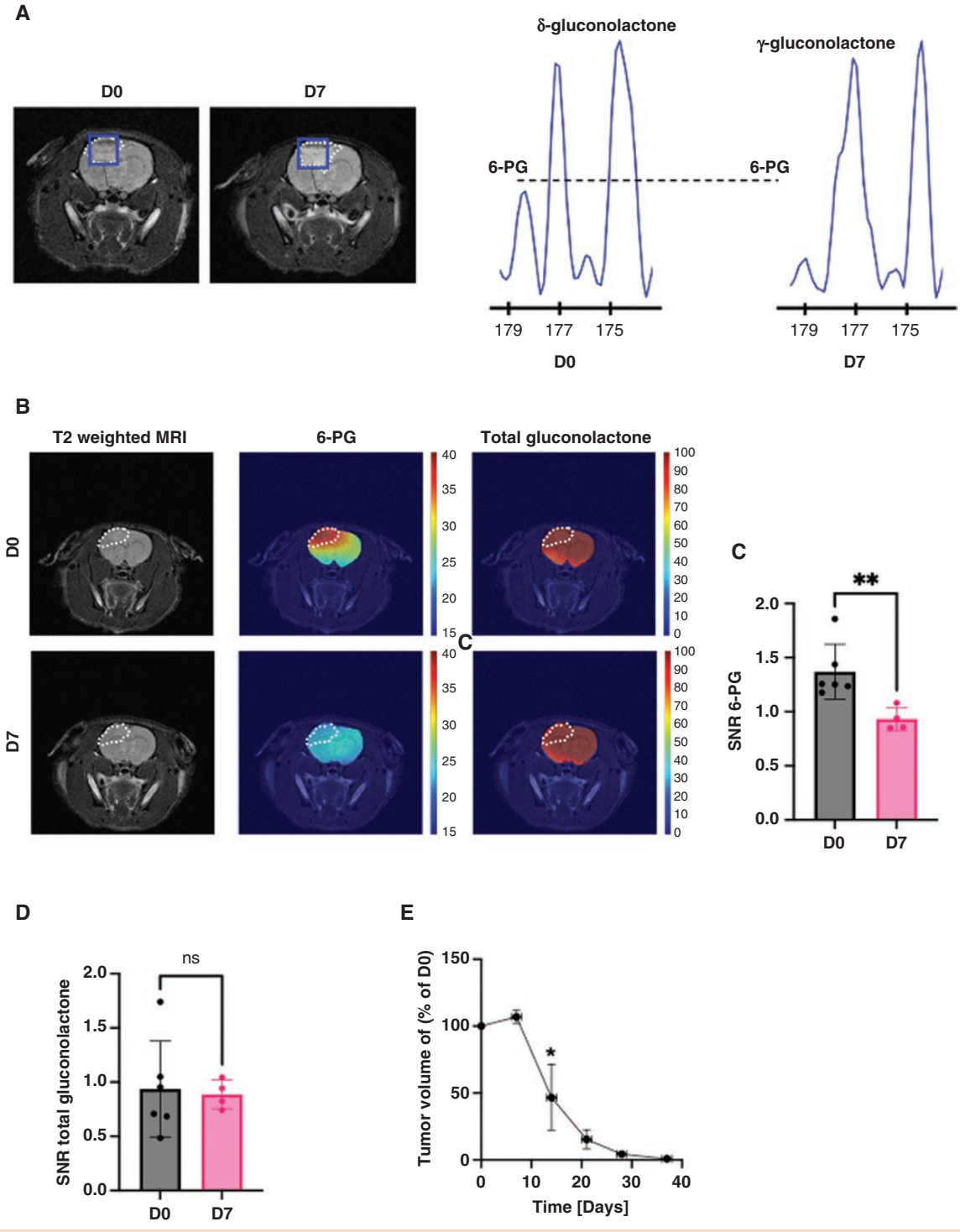

Figure 5. Hyperpolarized δ-[1-^{13}C]-gluconolactone can be used to monitor early response to therapy in oligodendrogliomas in vivo. (A) Representative 2D echo-planar spectroscopic imaging data showing the T2-weighted MRI (left) and corresponding ^{13}C-MR spectra (right) from tumor voxels in a rat bearing an orthotopic BT88 tumor before (day 0, D0) and after (day 7, D7) treatment with 6-thio-dG. The tumor region is contoured by white dotted lines. (B) Representative metabolic heatmaps from a rat bearing an orthotopic BT88 tumor before (top row, D0) and after (bottom row, D7) treatment with 6-thio-dG. For both rows, the left panel shows a T2-weighted MRI with the tumor contoured by white dotted lines. The middle panel shows the heatmap of the signal-to-noise ratio (SNR) of [1-^{13}C]-6-PG while the right panel shows the heatmap of the SNR of total [1-^{13}C]-gluconolactone overlaid over the T2-weighted MRI. Quantification of the SNR of [1-^{13}C]-6-PG in tumor normalized to contralateral normal brain (C) and the SNR of total [1-^{13}C]-gluconolactone (D) before (D0) and after (D7) treatment with 6-thio-dG in rats bearing orthotopic BT88 tumors. (E) Effect of 6-thio-dG on tumor volume. Tumor volume was measured by T2-weighted MRI and represented as a percentage of volume at D0. Studies were $n \geq 3$. * indicates statistical significance with $P < .05$. ** indicates statistical significance with $P < .01$. ns indicates a lack of statistical significance.

significant obstacle to liquid biopsy-based assessment of gliomas.[39,40] Hyperpolarized ^{13}C-MRS measures dynamic metabolic activity in a noninvasive manner. Imaging metabolic activity is important because it provides information on regulatory mechanisms or spatiotemporal changes in gene expression, by which the activity of key metabolic enzymes can be adjusted to meet the functional requirements of tumor cells.[41–43] Our studies highlight the ability of hyperpolarized δ-[1-^{13}C]-gluconolactone to provide a noninvasive readout of *TERT* expression, which is indispensable for tumor proliferation in oligodendrogliomas.

MRS is not routinely used to guide clinical decision-making, in part due to the lack of reproducible metabolic targets. Our studies demonstrate the reproducibility of imaging 6-PG production from hyperpolarized δ-[1-^{13}C]-gluconolactone in vivo. Furthermore, we demonstrate that hyperpolarized δ-[1-^{13}C]-gluconolactone has the potential to report on early response to therapy, which is challenging.[44,45] By providing an early readout of treatment response, prior to MRI-detectable alterations in tumor volume, hyperpolarized δ-[1-^{13}C]-gluconolactone can be used to stratify responders from nonresponders, thereby sparing nonresponsive patients the burden of ineffective treatment, toxicity, and healthcare costs. Accurate response assessment will also ensure that responsive patients continue to receive treatments that benefit them. Since clinical trials are expensive and recruiting oligodendroglioma patients is difficult due to the relative rarity of the disease,[46] preclinical studies such as those described in this manuscript are essential for clinical translation of hyperpolarized δ-[1-^{13}C]-gluconolactone to oligodendroglioma patients.

Our studies underscore the utility of imaging TERT-linked upregulation of G6PD activity in oligodendrogliomas. In a previous manuscript, we demonstrated that TERT upregulates G6PD, which is the rate-limiting enzyme of the PPP.[14] Mechanistically, we identified the sirtuin SIRT2 as a novel intermediary in the upregulation of G6PD by TERT.[14] Specifically, SIRT2 silencing downregulated G6PD activity in TERT+ cells and, conversely, SIRT2 overexpression restored G6PD activity in TERT– cells.[14] We leveraged this mechanistic information to show that 6-PG production from hyperpolarized [U-^{13}C, U-^{2}H]-glucose is a metabolic biomarker of TERT in oligodendrogliomas.[14] However, the short T1 (~14 seconds) of hyperpolarized [U-^{13}C, U-^{2}H]-glucose limits clinical applicability due to the technical challenges of transferring the hyperpolarized glucose solution from the polarizer to the patient within this short lifetime of polarization. To address this limitation, in the current study, we identify hyperpolarized δ-[1-^{13}C]-gluconolactone as an alternate agent for in vivo imaging of TERT in oligodendrogliomas. Specifically, we show that doxycycline-inducible TERT silencing downregulates G6PD activity and concomitantly downregulates 6-PG production from hyperpolarized δ-[1-^{13}C]-gluconolactone, effects that can be normalized by rescuing TERT expression via doxycycline removal. Having linked TERT expression to G6PD activity, we demonstrate that imaging G6PD activity using hyperpolarized δ-[1-^{13}C]-gluconolactone provides an early readout of response to telomerase inhibition in rats bearing patient-derived oligodendrogliomas. Collectively, our studies suggest that hyperpolarized δ-[1-^{13}C]-gluconolactone has the potential to assess, albeit indirectly, TERT expression and response to therapy in vivo.

A potential limitation of our study is the lack of information on the temporal evolution of hyperpolarized δ-[1-^{13}C]-gluconolactone metabolism in vivo. Our studies were focused on assessing the timing of 6-PG production relative to MRI-detectable volumetric alterations in rats bearing orthotopic oligodendrogliomas. Indeed, our studies show that 6-PG production from hyperpolarized δ-[1-^{13}C]-gluconolactone is reduced within 7 days of 6-thio-dG treatment, a timepoint when anatomical alterations are not observed on MRI. Future studies that longitudinally monitor hyperpolarized δ-[1-^{13}C]-gluconolactone metabolism at multiple timepoints before and after treatment are needed to pinpoint the earliest timepoint at which a drop in 6-PG production can be observed and determine the temporal evolution of 6-PG production relative to MRI-detectable tumor volume.

Another potential limitation of our study is the lack of data demonstrating the feasibility of imaging hyperpolarized δ-[1-^{13}C]-gluconolactone metabolism in human patients. Hyperpolarized ^{13}C-MRS studies in human glioma patients are expensive and beyond the scope of the current study. However, several factors point to the translational potential of hyperpolarized δ-[1-^{13}C]-gluconolactone. The T1 of hyperpolarized δ-[1-^{13}C]-gluconolactone at 3T is ~32 seconds,[19] a value that is significantly longer than that of hyperpolarized glucose and is comparable to that of hyperpolarized [2-^{13}C]-pyruvate (~39 seconds).[18] Importantly, our studies indicate that 6-PG production from hyperpolarized δ-[1-^{13}C]-gluconolactone can be reproducibly observed in the normal brain, thereby attesting to its ability to penetrate the blood-brain barrier.[19] Furthermore, the use of gluconolactone as a food additive at concentrations of 50 mM,[47] and the absence of adverse reactions in our studies at a concentration of 37.8 mM, minimize concerns regarding toxicity. Optimization of the hyperpolarized preparation, the use of higher magnetic fields during polarization and the application of denoising algorithms during post-processing could further improve the SNR of hyperpolarized δ-[1-^{13}C]-gluconolactone metabolism in future in vivo studies.[17,18]

In summary, our studies identify hyperpolarized δ-[1-^{13}C]-gluconolactone as a novel agent for imaging TERT expression in oligodendrogliomas. Clinical translation of hyperpolarized δ-[1-^{13}C]-gluconolactone has the potential to provide a readout of tumor burden and response to therapy in oligodendroglioma patients.

Keywords

hyperpolarized ^{13}C imaging | magnetic resonance spectroscopy | oligodendrogliomas | pentose phosphate pathway | TERT

Funding

Department of Defense (W81XWH201055315), National Institutes of Health (R01CA239288).

Acknowledgments

We thank Dr. Costello for the SF10417 model, and Dr. Luchman and Dr. Cairncross for the BT54 and BT88 models. We thank Will Byrne for technical support in the UCSF Preclinical MR laboratory. We acknowledge technical support from the National Institutes of Health-supported Hyperpolarized MRI Technology Resource Center.

Conflict of interest statement

The authors have no conflicting interests to disclose.

Authorship statement

Designed cell and in vivo experiments: G.B. & P.V., Synthesized δ-[1-^{13}C]-gluconolactone: C.T., Assisted with cell study: A.M.G., Performed cell experiments: G.B. & P.V., Performed in vivo experiments: G.B., Wrote manuscript and revision: G.B. & P.V., Conceived studies: P.V., Secured funding: P.V.

References

1. Hanahan D, Weinberg RA. Hallmarks of cancer: The next generation. *Cell*. 2011;144(5):646–674.
2. Shay JW, Wright WE. Telomeres and telomerase: Three decades of progress. *Nat Rev Genet*. 2019;20(5):299–309.
3. Bell RJ, Rube HT, Xavier-Magalhaes A, et al. Understanding TERT promoter mutations: A common path to immortality. *Mol Cancer Res*. 2016;14(4):315–323.
4. Bell RJ, Rube HT, Kreig A, et al. Cancer. The transcription factor GABP selectively binds and activates the mutant TERT promoter in cancer. *Science*. 2015;348(6238):1036–1039.
5. Mancini A, Xavier-Magalhaes A, Woods WS, et al. Disruption of the beta1L Isoform of GABP reverses glioblastoma replicative immortality in a TERT promoter mutation-dependent manner. *Cancer cell*. 2018;34(3):513–528.e8.
6. Louis DN, Perry A, Wesseling P, et al. The 2021 WHO Classification of Tumors of the Central Nervous System: A summary. *Neuro-oncology*. 2021;23(8):1231–1251.
7. Killela PJ, Reitman ZJ, Jiao Y, et al. TERT promoter mutations occur frequently in gliomas and a subset of tumors derived from cells with low rates of self-renewal. *Proc Natl Acad Sci USA*. 2013;110(15):6021–6026.
8. Arita H, Narita Y, Fukushima S, et al. Upregulating mutations in the TERT promoter commonly occur in adult malignant gliomas and are strongly associated with total 1p19q loss. *Acta Neuropathol*. 2013;126(2):267–276.
9. Mender I, Gryaznov S, Dikmen ZG, Wright WE, Shay JW. Induction of telomere dysfunction mediated by the telomerase substrate precursor 6-thio-2′-deoxyguanosine. *Cancer Discov*. 2015;5(1):82–95.
10. Sengupta S, Sobo M, Lee K, et al. Induced telomere damage to treat telomerase expressing therapy-resistant pediatric brain tumors. *Mol Cancer Ther*. 2018;17(7):1504–1514.
11. Mender I, Gryaznov S, Shay JW. A novel telomerase substrate precursor rapidly induces telomere dysfunction in telomerase positive cancer cells but not telomerase silent normal cells. *Oncoscience*. 2015;2(8):693–695.
12. Mender I, LaRanger R, Luitel K, et al. Telomerase-mediated strategy for overcoming non-small cell lung cancer targeted therapy and chemotherapy resistance. *Neoplasia*. 2018;20(8):826–837.
13. Stincone A, Prigione A, Cramer T, et al. The return of metabolism: Biochemistry and physiology of the pentose phosphate pathway. *Biol Rev Camb Philos Soc*. 2015;90(3):927–963.
14. Viswanath P, Batsios G, Ayyappan V, et al. Metabolic imaging detects elevated glucose flux through the pentose phosphate pathway associated with TERT expression in low-grade gliomas. *Neuro-oncology*. 2021;23(9):1509–1522.
15. Viswanath P, Batsios G, Mukherjee J, et al. Non-invasive assessment of telomere maintenance mechanisms in brain tumors. *Nat Commun*. 2021;12(1):92.
16. Ruiz-Rodado V, Brender JR, Cherukuri MK, Gilbert MR, Larion M. Magnetic resonance spectroscopy for the study of cns malignancies. *Prog Nucl Magn Reson Spectrosc*. 2021;122:23–41.
17. Viswanath P, Li Y, Ronen SM. C-13 hyperpolarized MR spectroscopy for metabolic imaging of brain tumors. In: Pope WB, ed. *Glioma Imaging: Physiologic, Metabolic, and Molecular Approaches*. Cham: Springer International Publishing; 2020:191–209.
18. Kurhanewicz J, Vigneron DB, Ardenkjaer-Larsen JH, et al. Hyperpolarized (13)C MRI: Path to clinical translation in oncology. *Neoplasia*. 2019;21(1):1–16.
19. Batsios G, Taglang C, Cao P, et al. Imaging 6-phosphogluconolactonase activity in brain tumors in vivo using hyperpolarized δ-[1-(13)C] gluconolactone. *Front Oncol*. 2021;11:589570.
20. Moreno KX, Harrison CE, Merritt ME, et al. Hyperpolarized delta-[1-(13) C]gluconolactone as a probe of the pentose phosphate pathway. *NMR Biomed*. 2017;30(6):1–8.
21. Kou Y, Xu J, Cao Y, et al. Gluconolactone induces cellulase gene expression in cellulolytic filamentous fungus Trichoderma reesei. *RSC Adv*. 2014;4(68):36057–36063.
22. Rohatgi N, Guðmundsson S, Rolfsson O. Kinetic analysis of gluconate phosphorylation by human gluconokinase using isothermal titration calorimetry. *FEBS Lett*. 2015;589(23):3548–3555.
23. Kelly JJ, Blough MD, Stechishin OD, et al. Oligodendroglioma cell lines containing t(1;19)(q10;p10). *Neuro-oncology*. 2010;12(7):745–755.
24. Jones LE, Hilz S, Grimmer MR, et al. Patient-derived cells from recurrent tumors that model the evolution of IDH-mutant glioma. *Neurooncol Adv*. 2020;2(1):vdaa088.
25. Izquierdo-Garcia JL, Viswanath P, Eriksson P, et al. IDH1 mutation induces reprogramming of pyruvate metabolism. *Cancer Res*. 2015;75(15):2999–3009.
26. Viswanath P, Radoul M, Izquierdo-Garcia JL, et al. Mutant IDH1 gliomas downregulate phosphocholine and phosphoethanolamine synthesis in a 2-hydroxyglutarate-dependent manner. *Cancer Metabol*. 2018;6:3.
27. Viswanath P, Radoul M, Izquierdo-Garcia JL, et al. 2-hydroxyglutarate-mediated autophagy of the endoplasmic reticulum leads to an unusual downregulation of phospholipid biosynthesis in mutant IDH1 gliomas. *Cancer Res*. 2018;78(9):2290–2304.
28. Batsios G, Taglang C, Tran M, et al. Deuterium metabolic imaging reports on TERT expression and early response to therapy in cancer. *Clin Cancer Res*. 2022;28(16):3526–3536.
29. Mender I, Shay JW. Telomerase Repeated Amplification Protocol (TRAP). *Bio Protoc*. 2015;5(22):e1658.
30. Kim NW, Wu F. Advances in quantification and characterization of telomerase activity by the telomeric repeat amplification protocol (TRAP). *Nucleic Acids Res*. 1997;25(13):2595–2597.

31. Rognstad R. Rate-limiting steps in metabolic pathways. *J Biol Chem.* 1979;254(6):1875–1878.
32. Fell DA. Enzymes, metabolites and fluxes. *J Exp Bot.* 2005;56(410):267–272.
33. Shukla-Dave A, Obuchowski NA, Chenevert TL, et al. Quantitative imaging biomarkers alliance (QIBA) recommendations for improved precision of DWI and DCE-MRI derived biomarkers in multicenter oncology trials. *JMRI.* 2019;49(7):e101–e121.
34. Dandekar M, Tseng JR, Gambhir SS. Reproducibility of 18F-FDG microPET studies in mouse tumor xenografts. *J Nucl Med.* 2007;48(4):602–607.
35. Serrao EM, Rodrigues TB, Gallagher FA, et al. Effects of fasting on serial measurements of hyperpolarized [1-(13) C]pyruvate metabolism in tumors. *NMR Biomed.* 2016;29(8):1048–1055.
36. McGuire SA, Wijtenburg SA, Sherman PM, et al. Reproducibility of quantitative structural and physiological MRI measurements. *Brain Behav.* 2017;7(9):e00759.
37. Hasanau T, Pisarev E, Kisil O, et al. Detection of TERT promoter mutations as a prognostic biomarker in gliomas: Methodology, prospects, and advances. *Biomedicines.* 2022;10(3):728.
38. Diplas BH, Liu H, Yang R, et al. Sensitive and rapid detection of TERT promoter and IDH mutations in diffuse gliomas. *Neuro-oncology.* 2019;21(4):440–450.
39. Soffietti R, Bettegowda C, Mellinghoff IK, et al. Liquid biopsy in gliomas: a RANO review and proposals for clinical applications. *Neuro-oncology.* 2022;24(6):855–871.
40. Wan JCM, Massie C, Garcia-Corbacho J, et al. Liquid biopsies come of age: Towards implementation of circulating tumour DNA. *Nat Rev Cancer.* 2017;17(4):223–238.
41. Grimbs S, Selbig J, Bulik S, Holzhütter H-G, Steuer R. The stability and robustness of metabolic states: Identifying stabilizing sites in metabolic networks. *Mol Syst Biol.* 2007;3(1):146.
42. Metallo CM, Vander Heiden MG. Understanding metabolic regulation and its influence on cell physiology. *Mol Cell.* 2013;49(3):388–398.
43. Watson E, Yilmaz LS, Walhout AJM. Understanding metabolic regulation at a systems level: Metabolite sensing, mathematical predictions, and model organisms. *Annu Rev Genet.* 2015;49(1):553–575.
44. Ellingson BM, Bendszus M, Boxerman J, et al; Jumpstarting Brain Tumor Drug Development Coalition Imaging Standardization Steering Committee. Consensus recommendations for a standardized Brain Tumor Imaging Protocol in clinical trials. *Neuro-oncology.* 2015;17(9):1188–1198.
45. Lowe SR, Sattur MG, Vogelbaum MA. Chapter 38 - Response assessment in neuro-oncology criteria: overview and future directions. In: Newton HB, ed. *Handbook of Neuro-Oncology Neuroimaging*, 3rd edn. Cambridge, MA: Academic Press; 2022:491–499.
46. Aldape K, Brindle KM, Chesler L, et al. Challenges to curing primary brain tumours. *Nat Rev Clin Oncol.* 2019;16(8):509–520.
47. Whitaker JR VA, Wong DWS. *Handbook of Food Enzymology.* Boca Raton: CRC Press; 2002.